Hardness Variation and Cyclic Crystalline-Amorphous Phase Transformation in a CuZr Alloy during Ball Milling

By

David Taylor Schoen

Submitted to the Department of Materials Science and Engineering in Partial Fulfillment of the Requirements for the Degree of

Bachelor of Science

at the

Massachusetts Institute of Technology

June 2005

Signature of Author .....
Department of Materials Science and Engineering
May 11, 2005

Certified By .....
Christopher A. Schuh
Danae and Vasilios Salapatas Assistant Professor of Metallurgy
Thesis Supervisor

Accepted By .....
Donald R. Sadoway
John F. Elliott Professor of Materials Chemistry
Chairman, Undergraduate Thesis Committee

Hardness Variation and Cyclic Crystalline-Amorphous Phase Transformation in a CuZr Alloy during Ball Milling

By

David Schoen

Submitted to the Department of Materials Science and Engineering on May 11, 2005 in Partial Fulfillment of the Requirements for the Degree of Bachelor of Science at the Massachusetts Institute of Technology

ABSTRACT

The hardness and percent crystallinity of $Cu_{33}Zr_{67}$ powder samples are measured through several cycles of a cyclic phase transformation during ball milling. Each are found to cycle with a period of approximately 320 minutes. Although significant chemical contamination was found in the milled specimens, the results shed some light on mechanical alloying theory and favor interpreting mechanical alloying as a driven alloys process.

Thesis Supervisor: Christopher Schuh
Title: Danae and Vasilios Salapatas Assistant Professor of Metallurgy

Table of Contents

List of Figures

List of Tables

1. Introduction and Review

1.1 Overview

Materials far from equilibrium are of growing importance for a wide range of technologies, and research into them is among the most exciting being pursued today. Among some of the important far from equilibrium materials are amorphous and nanocrystalline metals. These materials have a wide range of unique and useful properties. Amorphous metals have been used for some time in electrical transformers due to their unique magnetic properties; however, amorphous metals and nanocrystalline metals have a large set of impressive mechanical properties as well. They are much stronger than normal polycrystalline metals and can exhibit super plasticity. Recent progress towards practically producing amorphous and nanocrystalline metals in the bulk, combined with their unique set of properties, may soon make them an important new class of structural material.

There are many different processing routes to produce these materials, including high speed cooling, casting of substances with complex chemical composition, and various forms of film deposition. One particularly interesting processing technique for the development of far from equilibrium materials is mechanical alloying. Mechanical alloying is essentially mixing by repeated high intensity plastic deformation. Mechanical alloying has been widely used for making both amorphous and nanocrystalline metals. Generally in two component systems these processes first generate composites with some characteristic length scale of phase separation. Further processing refines this length scale. When it reaches atomic scale dimensions, a variety of structures may be produced depending on the chemical makeup of the processed material.

There is some controversy as to how mechanical alloying produces metastable structures. It has been proposed that the introduction of defects from the mechanical deformation speeds

interdiffusion, or that these defects store energy in the crystalline phase until the crystalline phase is at a higher energy than a competing metastable phase. It has also been proposed that specimens being mechanically alloyed can be viewed as thermodynamically driven systems in which atomic movement induced by repeated deformation events establishes an effective temperature. Most of these theories implicitly assume that systems being mechanically alloyed will reach some steady state structure which is characteristic of the relevant processing variables.

One phenomenon which seems to overthrow this assumption has been repeatedly observed during ball milling, which is one mechanical alloying process. In certain systems with certain processing intensities, it has been observed that the first solid state amorphization is followed by transformation to a crystalline phase. With even more processing the newly formed crystalline phase will transform back into an amorphous one. Further processing leads to more transformations. These cyclic transformations have been difficult to explain.

This study was undertaken to investigate this problem. The rest of this section consists of a technical review of mechanical alloying, the ball milling process, and the work done on the cyclic transformations so far. It ends with the statement of this particular study's goals and the particular question it seeks to answer. Section 2 outlines the experiments performed, section 3 offers the results of these experiments and discusses them, and the last section summarizes the conclusions of the study.

1.2 Mechanical Alloying Theory

Mechanical alloying was first developed in the 1960's as a method for producing dispersion strengthened nickel alloys. During the 1980's mechanical alloying was used to produce amorphous materials from intermetallic compounds and blended elemental mixtures.

Subsequently, the technique has been used for producing a wide range of novel metastable materials[1]. Mechanical alloying processes produce a composite microstructure through repeated cold welding and fracture or cutting whose characteristic length scale of phase separation refines. Long processing times reduce this length scale to atomic dimensions, and at this point atomic scale mixing occurs.

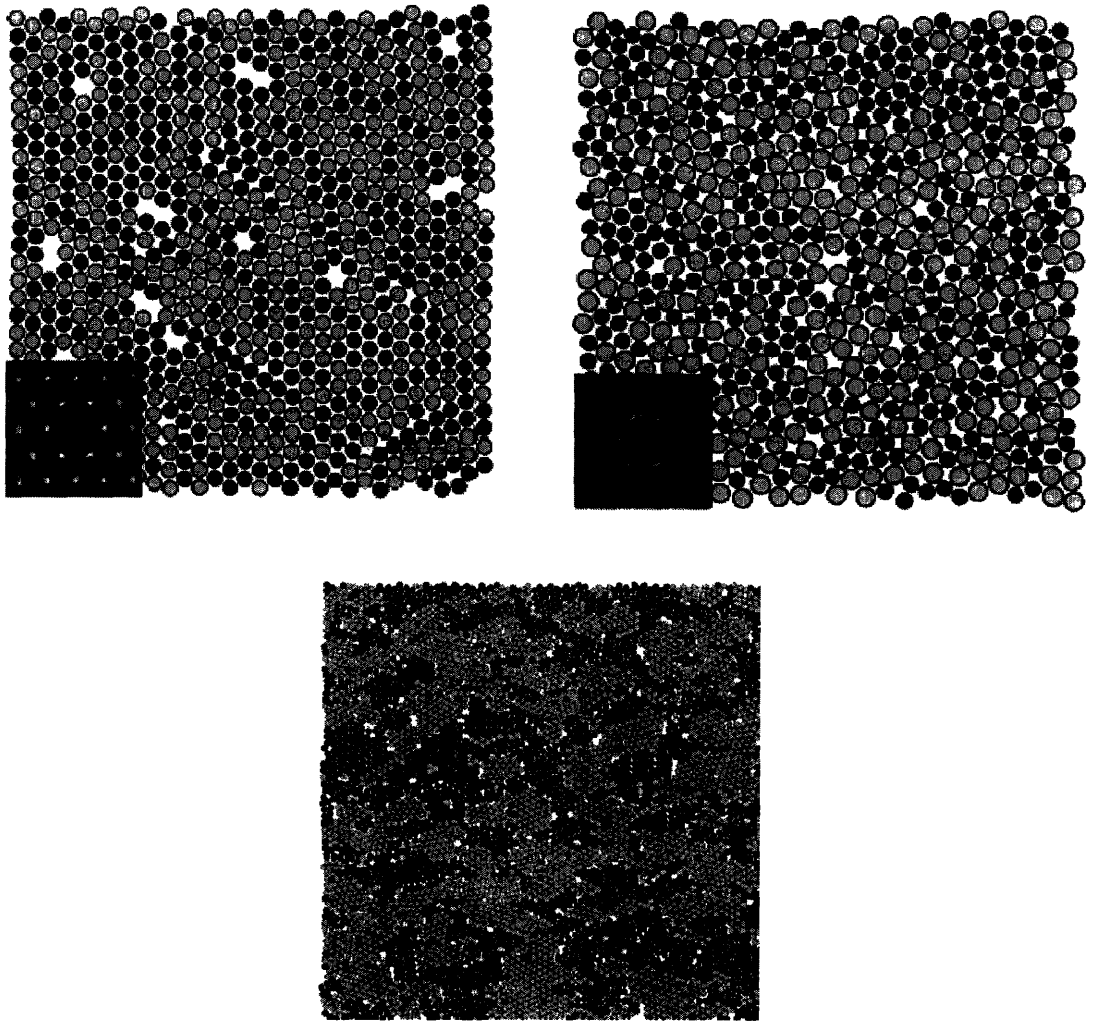

Figure 1
Images produced in a simulation of mechanical alloying with different chemical compositions. Moving clockwise from the upper left, the first picture was produced starting with two elements, light and dark, with a zero heat of mixing and no atomic radius mismatch. The second was produced with a zero heat of mixing and a significant atomic size mismatch. The third was produced with a negative heat of mixing and no atomic size mismatch.

After atomic scale mixing, a variety of end products have been predicted and observed: metastable solid solutions[2], nanosegregated composites, and amorphous alloys[1]. According to a set of simulations carried out by Schuh and Lund[3], there are two important factors determining the nature of the final product: the heat of mixing and the atomic radius mismatch. The results of this study are shown in Figure 1. Pairs of substances with 0 or negative heats of mixing will produce solid solutions and amorphous alloys. Of these pairs substances with small atomic radius mismatches will produce solid solutions, while substances with large mismatches will generate amorphous materials. Nanosegregated composites are produced in materials with positive heats of mixing. These end products have been observed in a variety of experimental studies, and also in simulation.

There is still no clear consensus about how mechanical alloying produces nanocrystalline and amorphous structures, although there are currently two popular theories being considered which are relevant to this study. The first model claims that energy is stored in materials being mechanically alloyed in the form of crystal defects. Kinetic barriers inhibit formation of a stable non-defected phase, but the materials can relax to structures of intermediate energy, such as amorphous and nanocrystalline solid solution phases. Models which attempt to explain the amorphization with an appeal to the destabilization of the crystalline phase in favor of the amorphous one are of the first variety. In support of these models it has been shown that mechanical alloying by ball milling can store remarkable amounts of energy in milled samples, up to 50% of the enthalpy of fusion[4]. It is plausible that these processes could raise the internal energy of an alloyed system above the internal energy of amorphous and nanocrystalline phases. An excellent discussion of these models is included in the review on mechanical alloying written by Suryanarayana[1].

The second model considers mechanical alloying to be among the driven alloy processes, which also include the irradiation of materials. Driven alloy theory proposes that these processes have some effective temperatures, and that different phases can be in dynamic equilibrium at different effective temperatures. Driven alloy theory is appropriate for processes which cause large amounts of random atomic movement. The canonical system treated by driven alloy theory is that of irradiated materials, where incident particles collide with atoms in the lattice and cause a cascade of random atomic motion. The number and energy of these collisions generates a characteristic processing intensity which can be correlated with an effective processing temperature. This effective temperature determines which phases are present in the material at the end of irradiation. Mechanical alloying seems like a good candidate for treatment with driven alloy theory. Plastic deformation causes many small scale shearing events which promote extensive relative atomic motion. The number and magnitude of these straining events should in principle determine a processing intensity and effective temperature. As in irradiated materials, this effective temperature may determine the phases present in dynamic equilibrium during the process. A review of driven alloys was written by Martin and Bellon[5].

1.3 Ball Milling Review

Ball milling is one process for mechanical alloying. A ball mill is a device which agitates vials containing milling balls and powder specimens. Collisions between the balls, vial, and powder cause plastic deformation, cold welding, and fracture in the processed powders. When powder particles of two different phases are deformed and cold welded together, a lamellar like composite of the two phases is formed. When a composite particle is welded to another composite particle and deformed, a particle with smaller lamellae is formed. These

particles fracture, and cold weld to other particles. As this process is repeated thousands of times, the size scale of the phase separation in the powder particles decreases. At very long times, this size scale reaches atomic dimensions and mechanical alloying occurs. The refinement of size scale in a sample system, $Co_{25}Ti_{75}$, can be seen in Figure 2 taken from a study by El-Eskandaranay[6].

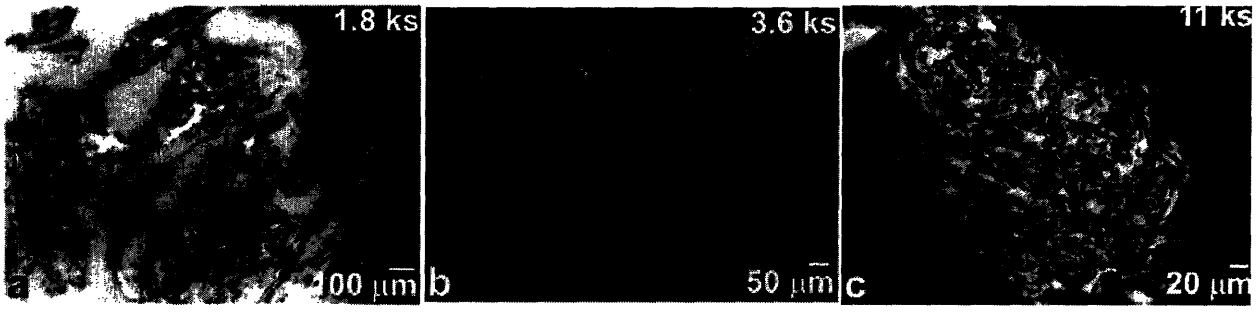

Figure 2
SEM images of powder particles at different times during ball milling. The lengthscale of the features pictured decreases over time.

There are several types of ball mill: attritor mills, simple rotational mills, vibratory mills, and planetary mills. These mills are illustrated in Figure 3. In an attritor mill a large vial filled with milling balls is agitated by steel shafts rotated through it. In a simple rotational mill, a cylindrical vial containing balls is rotated. Below a critical velocity, balls fall off one face of the vial to the bottom, leading to collisions. Attritor mills process powder mainly through shearing caused by balls sliding past one another. The intensity of the process in a simple rotational mill is limited by the critical speed, above which the milling balls are held on the outside of the vial and do not collide with the powder. Processing in these mills is considered low intensity.

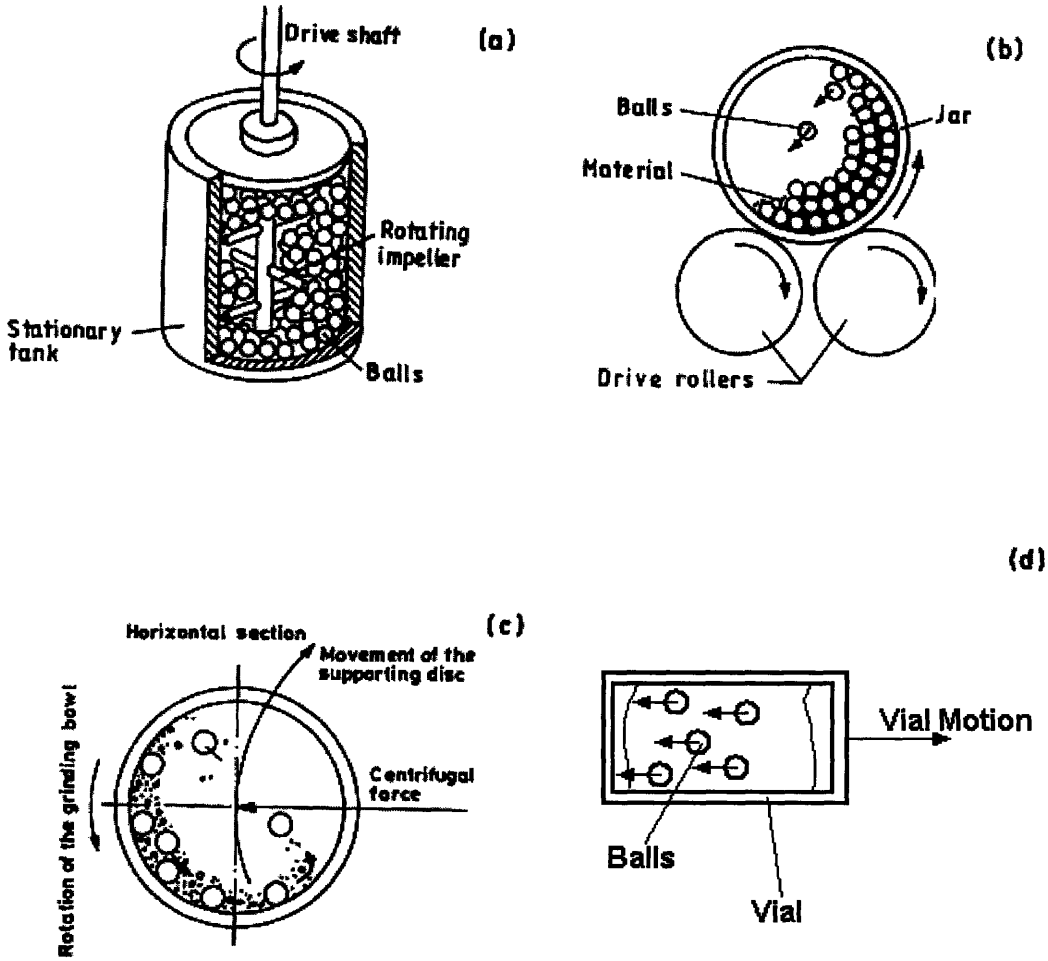

Figure 3
Schematics of different kinds of ball mill[13]. (a) is an attritor mill, (b) a tumbler or simple rotational mill, (c) is a planetary mill, and (d) is a vibratory mill.

The vibratory "shaker" mill and planetary mill, most commonly the Spex 8000M vibratory mill and Fritsch G5 or G7 planetary ball mill are the ones primarily used for mechanical alloying experiments. They are both high energy mills, as compared to the attritor and simple rotational mills. High energy mills produce samples in faster times, and have much higher processing intensities than low energy mills, although they hold smaller quantities of material.

A Fritsch planetary mill holds a set of vials on a rotating disc. The vials themselves also rotate. The rotation of the larger disc causes centripetal acceleration in the milling balls, while the rotation of the vials prevents them from merely sitting on the outsides of the vials. The planetary rotation avoids the problem of critical velocity encountered in a simple rotational mill. The speed of the larger disc controls the impact velocity of the balls with the sides of the vials, while the speed of the smaller disc controls the impact frequency[7]. On a Fritsch G5, the speed of the two vials is coupled but controllable, while on a G7 they are independently adjustable. The motion of the balls in a planetary mill has been modeled[8].

A Spex 8000M vibratory mill holds one vial in an arm which oscillates along several axes at a very high frequency. The frequency of this oscillation is not adjustable without modification to the mill. The motion of the balls in a vibratory mill is very complicated, since both direct collisions with the top and bottom of the vial as well as glancing collisions with the sides occur[9]. For these reasons the impact velocity and frequency are more difficult to determine and control in a shaker mill, although the impact velocity is at least proportional to the vial's velocity, and the frequency proportional to the vial's oscillatory frequency.

There are several important stochastic variables which complicate analysis of the ball milling process in both mills. The amount of deformation achieved for any one ball impact depends strongly on how much powder is trapped between the balls, whether the impact is between the ball and the wall of the vial or between two balls, and whether the collision is direct or glancing. In addition, collisions can cause large local heating, so the process cannot be regarded as isothermal[10].

There are many processing variables which can be controlled in a ball milling experiment: the material used for the vial and the balls, the size and number of balls, the amount

of powder used, the ball to powder weight ratio, the volume filling fraction of the vial, processing time, average temperature, and for the planetary mills the rotation speeds of the disc and vials. Each of these variables affects the process, but only some of them affect the relevant processing intensity.

The first relevant parameter is the volume filling fraction, which controls the balls' mean free path and the dominant deformation mechanism. For small filling fractions, the dominant deformation mechanisms are collisions between the balls and the walls of the vials which cause fast severe plastic deformation in the processed specimens[11]. When the filling fraction becomes large the balls are not free to move far enough to collide with each other, and the dominate deformation mechanism becomes shear deformations from balls sliding over one another. The sliding mode is less intense than the collision mode, and is therefore less preferable for mechanical alloying. Generally small filling fractions are used in ball milling for mechanical alloying.

For ball milling with small filling fractions, it has been demonstrated by several investigators that the important parameter affecting the processing intensity is the power transferred from the mill to the processed specimens[12].

$$P_I = E_I \cdot F_I \qquad (1)$$

P_I is the processing power, E_I is the energy per impact, and F_I is the impact frequency. For balls perfectly coated with powder, the impacts have been demonstrated to be nearly perfectly inelastic. Given this assumption:

$$E_I = \tfrac{1}{2} \cdot m_{ball} \cdot v_{ball}^{\,2} \qquad (2)$$

m_{ball} is the mass of the milling balls, and v_{ball} is their velocity at impact. Models for ball motion in a planetary mill have been used to predict the impact frequency and the ball velocity as

functions of the angular velocities of the vial and disc[7]. For the planetary mills, therefore, power can be calculated. As was previously stated, the SPEX mills are more difficult to model, so determining the processing power is difficult. It can be roughly accomplished by correlating experimental results in a reference system obtained on a planetary mill with those on a Spex mill[13].

1.4 Cyclic Amorphous Crystalline Phase Change

In 1997 El-Eskandarany observed a phenomenon difficult to explain with driven alloy theory or a defect accumulation model[14]. It was found that high energy milling of elemental $Co_{75}Ti_{25}$ powders produced a cyclic transformation between a disordered bcc Co_3Ti solid solution and an amorphous specimen. Two full cycles were ultimately observed, and the identity of the phases was verified with XRD, DSC, and TEM[15]. Cyclic phase transformations have subsequently been observed in a variety of systems including $Cu_{33}Zr_{66}$[6], $Co_{50}Ti_{50}$[16], $Al_{50}Zr_{50}$[17]. A cyclic change has also been reported in elemental Co[18], but between FCC and HCP phases, not crystalline and amorphous. Devitrification induced by ball milling has also been observed in a variety of amorphous metals including $Zr_{65}A_{7.5}lNi_{10}Cu_{12.5}Pd_5$[19], $Al_{80}Fe_{20}$[20], $Ti_{75}Al_{25}$[21].

In the cyclic transformation experiments contamination was very carefully controlled, and was observed to increase slowly but monotonically. If it were playing a role in the cyclic transformations one would expect it to oscillate. The temperature of the process was also carefully controlled. For all his experiments El-Eskandarany monitored the temperature and interrupted the process periodically to insure it remained well below the Tg of the amorphous phase.

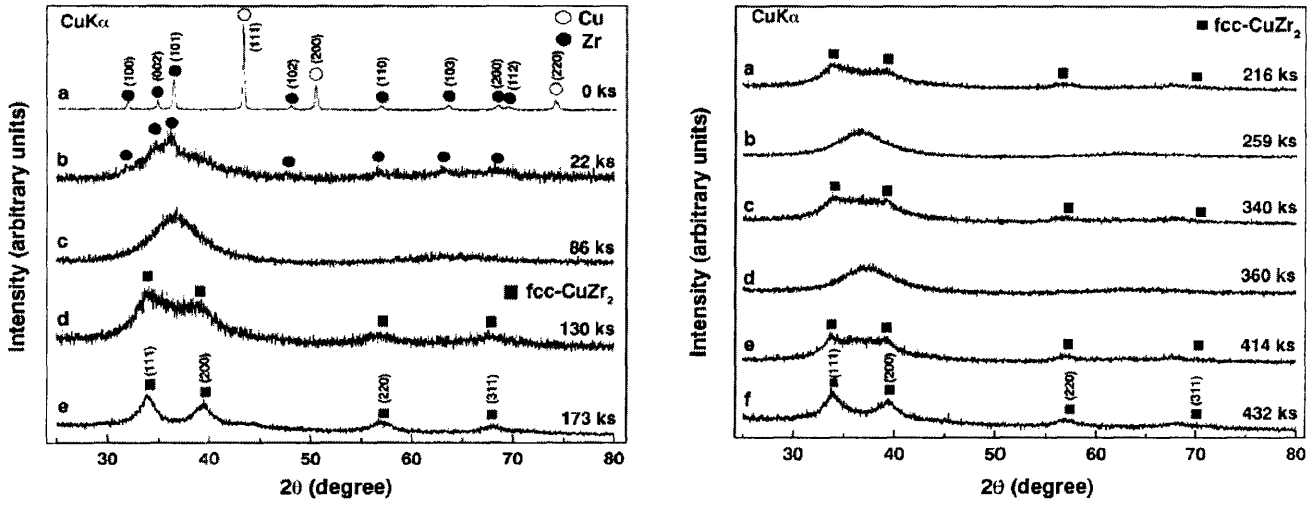

Figure 4
X-ray data obtained by El-Eskandarany during experiments[6] on the cyclic transformation in $Cu_{33}Zr_{67}$ for samples milled at different times. The time is written above each scan in kiloseconds, and crystal peaks are identified by marks above them.

One processing variable was observed to significantly affect the cyclic transformations. Higher rotational velocities in planetary mills, which are proportional to the processing intensity, were observed to lead to the cyclic transformation in several of the systems. Lower rotational velocities were observed to generate either an amorphous phase which did not cycle, or a composite of the amorphous phase and the elemental crystalline phases[6].

The existence of these cyclic transformations is a problem for both potential theories seeking to explain the creation of metastable structures in mechanically alloyed specimens. Each theory seems to predict that for some given processing intensity there should be one structure created by mechanical alloying. In order to be a viable explanation of mechanical alloying, each theory would have to offer a plausible account of how the cyclic transformations occur.

In one explanation offered in a paper by Sluiter and Kawazoe[22] which attempts to reconcile the defect accumulation model with the phenomenon, energy stored as defects in the milled powders is suggested to catalyze the change between the crystalline and amorphous

phases. The stored energy is assumed to dissipate during the phase change. Further milling stores energy in the new phase, and the change back is thereby catalyzed. This model can account for the dependency of the process on milling intensity, but predicts that the phase oscillation should be very heavily damped for physically reasonable values of stored energy. So far such heavy damping of the cyclic phase change has not been observed.

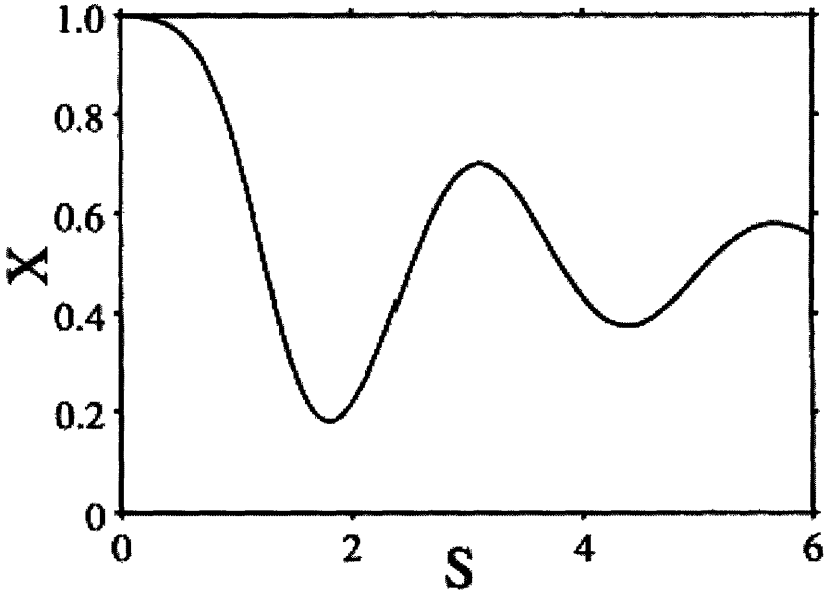

Figure 5
Damped phase oscillation predicted by Sluiter and Kawazoe[22]. X is the amorphous fraction, and S is a unitless time parameter.

There may also be an explanation consistent with driven alloy theory. It has been suggested that the phase change may be due to a variation in hardness during the milling process[23]. The phases obtained during ball milling have been found to be very dependant on the intensity of the milling process[7]. A harder powder will deform less for the same level of agitation, and hence will experience a lower intensity process. Therefore a hardness variation would also be a variation in the processing intensity, and varying hardness could lead to a time dependant promotion of one phase rather than the other.

1.5 Experimental Investigation of Hardness Variation

Although it has been suggested that a variation in mechanical properties may be part of an explanation of the cyclic phase transformations, and such a variation is to be expected, it has not yet been experimentally investigated. Most of the studies cited above use various techniques for probing the amorphous fraction of processed powders as a function of processing time in a variety of systems, and of establishing the identity of the phases formed through diffraction and DSC experiments.

Some variation is certainly to be expected. Hardness is generally a function of the microstructure of a specimen and the microstructure of these systems is heavily affected by the process. The exact nature of this variation could be very interesting. The discovery that the hardness cycles between two extremes with a period approximately equal to that of the cyclic phase change would bolster the explanation for the cyclic phase change appealing to a cyclic variation in processing intensity.

This study attempts to show how the hardness of specimens varies as a function of processing time in ball milling during cyclic phase transformations. In order to address this question a series of samples were ball milled for different times in a system in which cyclic transformations had been observed under the conditions in which they had been observed. The microstructure of these samples was characterized using x-ray diffraction, and their hardness was measured with nanoindentation. A discussion of the importance of these findings for mechanical alloying theory follows.

2. Experiment

2.1 Sample Preparation

A Spex 8000M shaker mill was used to produce $Cu_{33}Zr_{66}$ powders processed for different times through several cycles of a cyclic phase transformation. The $Cu_{33}Zr_{66}$ system was chosen because it is a well know glass former, the elements are innocuous and relatively cheap, and the cyclic transformation had been previously observed in it. The primary concerns for the design of this ball milling experiment were controlling chemical contamination, processing intensity, and processing time.

Several steps were taken to attempt to reduce chemical contamination in the milled specimens. Oxygen and nitrogen contamination is often a problem due to the exposure of fresh metal surfaces during deformation[1], and in a CuZr system the problem can be especially bad due to both of those elements' large affinities for oxygen. Collisions of the milling media with the sides of the vials will also cause small amounts of material to break off and mix in with the milled specimen[1]. This material is a source of iron contamination.

In order to mitigate contamination from the milling media and the vials, hardened tool steel vials and ball bearings were used. Hardened tool steel can often be used to significantly reduce the amount of iron contamination as compared to normal steel. Tungsten carbide balls and vials are also often used when contamination is a large concern, but they are dramatically more expensive.

In order to mitigate gaseous contamination the powders were packed under a controlled atmosphere in a VAC glove box with an attached oxygen filtration unit. Several times during the course of the experiment the quality of the atmosphere in the box was checked and found to be less than 5 ppm oxygen. The glovebox was shared, so for a time it was filled with a high purity argon atmosphere, and for a time it was filled with a high purity nitrogen atmosphere. After

being loaded with the specimen and the milling media the vials were sealed with a greased rubber gasket.

The cyclic phase transformations do not occur for low processing intensities[6]. The original experiments on ball milled CuZr were carried out on a Fritsch planetary ball mill, so in order to ensure that the phase transformations would occur using the shaker mill it was necessary to choose the processing parameters so as to match, at least approximately, those processing conditions in the original experiment. There are several important factors: the filling fraction, the size of the balls, and the ball to powder weight ratio.

For processes dominated by the same deformation events the relevant processing parameter is the impact power[7]. The power is given in terms of the energy of each impcact and the impact frequency by Equation (1):

$$P_I = E_I \cdot F_I \qquad (1)$$

The average impact energy is given in terms of the ball mass and velocity by equation (2):

$$E_I = \tfrac{1}{2} \cdot m_{ball} \cdot v_{ball}^{\,2} \qquad (2)$$

In a planetary mill the ball velocity and the collision frequency may be varied by changing the rotation speeds of the disc and the vial; however in a Spex mill both are determined by the vibration frequency of the vial which is not controllable. Therefore, in a Spex mill the only controllable parameter for determining the processing intensity is the ball size.

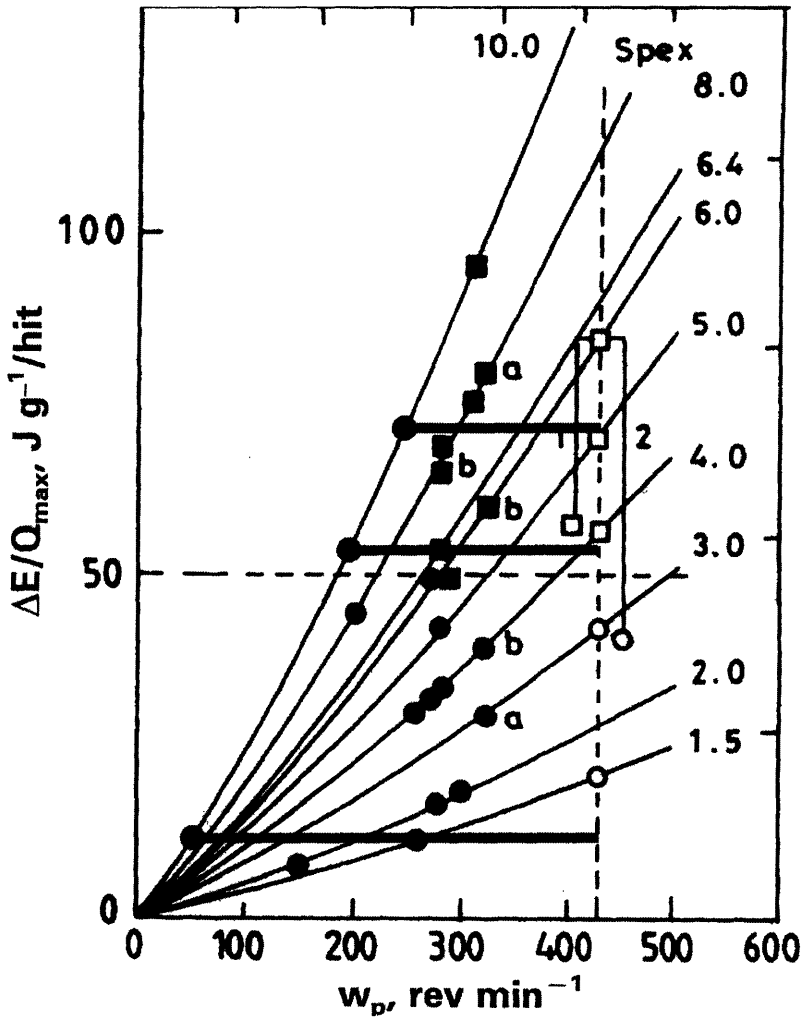

Figure 6
Plot of shock power versus revolutions per minute using balls of different size in a planetary ball mill and a vibratory mill[24]. The solid black diagonal lines are calculated values for a planetary mill with different ball diameters given in mm at the ends of the curves. The solid marks are experimental results for experiments done on Pd-Si system in a planetary mill. Circles correspond to crystalline phases and squares to amorphous ones. The hollow marks correspond to experiments on the same system done in a vibratory mill.

The exact physics of ball motion in a Spex mill are not well understood, so the average ball velocity and impact frequency are difficult to determine directly. It is possible to estimate the impact power by comparing the results of a mechanical alloying experiment in a reference system. Figure 6 shows the results of experiments on a Pd-Si system by Magini and Iasonna[24]. The diagonal lines show calculated energy per impact values in a planetary mill for balls of

different size and with different rotational velocities. The solid dots are experiments carried out in the Fritsch mill. The shapes represent the final phase obtained: circles are crystalline and the squares are amorphous. It can be seen that there is a critical processing power above which the samples produced were all amorphous. The open dots are for experiments carried out in the same system with a with a Spex mill, using balls of different diameters. There was a critical ball diameter above which all the samples produced were amorphous. The intensity of the Spex mill process can be roughly correlated with that of the planetary mill by assuming milling with balls of the critical diameter has the same power as the critical power in the planetary mill experiments. The processing powers for the other ball diameters can be calculated once this one reference point is known.

El-Eskandarany's experiments were performed using 10mm balls with rotational speeds of 1.1 min^{-1}, 3.3 min^{-1} and 4.2 min^{-1}. The cyclic phenomenon was observed for 3.3 min^{-1} and 4.2 min^{-1}, but not 1.1 min^{-1}. Using Figure 6 the processing power for each of these processes was plotted, and the correlating ball diameters for the same intensity experiments in a Spex mill estimated. 4.76 mm (3/16") diameter balls were used. In order to ensure that the dominant deformation events were collisions rather than sliding a small filling fraction of less than 1:10 was used. The ball to powder weight ratio is also important as it affects the impact events. A ball to powder weight ratio of 5:1 is typical, and was used for this experiment.

Samples processed for different times were gathered by running one vial continuously for a particular processing interval and then collecting its entire contents. Due to the small amount of sample in each vial, attempting to collect fractions of the sample at different times was impractical. Since the process for determining the intensity relied on some very rough estimates the period of the cycles to be observed in the experiment was not predictable. The period of the

cycles in El-Eskandarany's paper was 3000 minutes, so initially samples were taken every 300 minutes from 300 to 1800 minutes. Upon x-ray analysis there was clearly at least 1 full cycle, so a new set of samples were taken half way between the first set of samples. Ultimately, samples were taken at 600, 675, 750, 825, 900, 975, 1050, 1125, 1200, 1350, 1400, 1500, and 1800 minutes.

2.2 Microstructural Characterization with XRD

Microstructural analysis of the sample was carried out using x-ray diffraction. Tests were done with a Rigaku x-ray generator running at 60 kV and 300 mA, using Cu K_α radiation. A 185 mm Rigaku diffractometer was used with a 1 degree solar slit, a 1 degree diffraction slit, and a .5 mm receiving slit. Scans were run with a data interval of 0.02 degrees and a scan speed of 1 degree per minute.

X-ray peaks were decomposed using the non-linear optimization routines built into the program Jade 7. For samples with very high crystalline content the peaks were well separated and could be fit individually very successfully with pseudo-voight peak shapes and an iterative fitting routine. The samples with higher amorphous fractions could not be adequately analyzed with this technique due to heavy overlap between the very broad crystal peaks and the two amorphous peaks. In order to decompose these peaks a slightly more sophisticated peak fitting routine known as the Reitveld method was used[25]. In the Reitveld method, a physical model is used to predict peak positions and shapes. Instead of merely fitting the peak shapes individually, the optimization routine manipulates the parameters of the model to fit all the peaks from that phase together. The refinement process generally starts with a set of best guesses for the majority of the parameters and the background and any amorphous peaks, then one by one the

parameters are let to vary and the fit improves. When the structure of the material is known very accurately the Reitveld technique can produce a wide variety of information from an x-ray scan, and can decompose reliably overlapping peaks that less sophisticated peak fitting cannot.

The amorphous fraction of each sample was calculated from the decomposed peaks using a method put forward by Delogu, Cocco and Schifinni[26]. The ratio of the integrated intensity from the crystalline peaks to the total integrated intensity of the scan is plotted against the scattering vector squared, where the scattering vector $s = 4\pi\frac{\sin\theta}{\lambda}$, as shown in Figure 7. This plot follows a parabolic trend, whose y-intercept equals the crystal volume fraction in the sample.

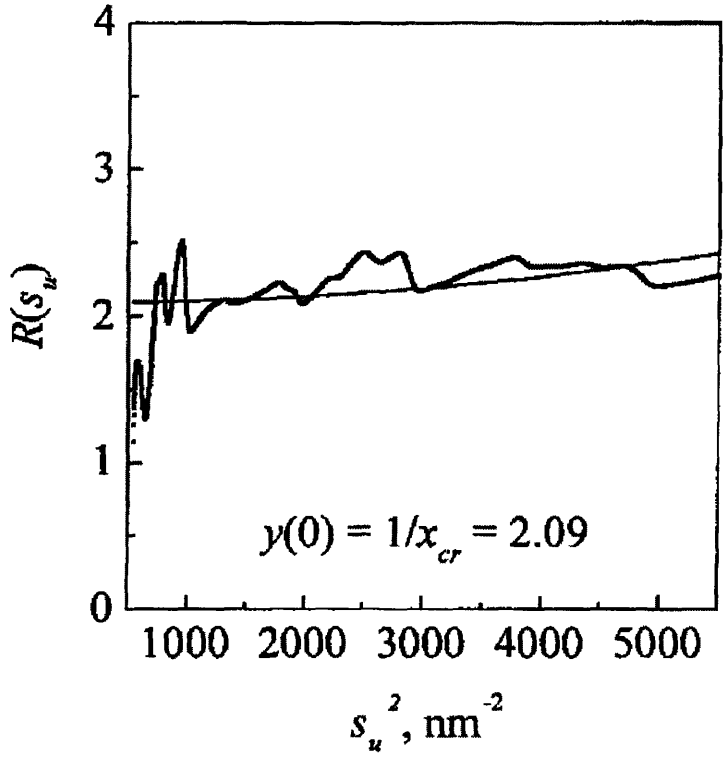

Figure 7
Example plot used for calculation of the crystalline fraction from an x-ray scan with method from Delogu, Schiffini, and Cocco[26]. The ratio of integrated crystalline intensity to total integrated intensity varies around a parabola. The extrapolated intersection of this parabola with the y-axis is the inverse of the crystalline phase fraction.

2.3 Hardness Testing

Hardness data were collected using a Hysistron nanoindenter. A nanoindenter was used because the powder specimens obtained were too fine for microhardness testing. Often the hardness of ball milled samples is measured only after the samples have been put through hot or cold isostatic pressing; however this process could have had a significant impact on the microstructure of the samples so would have obscured the relevant hardness values. Instead, the samples were mounted in a hard epoxy resin and polished to a 0.5 micron finish.

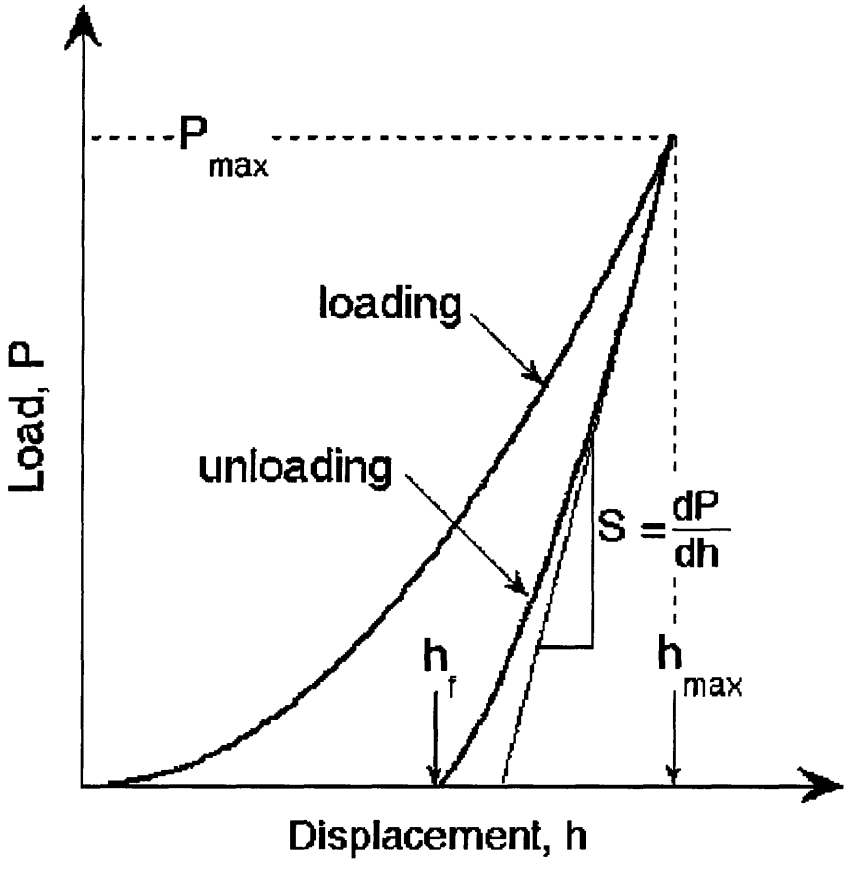

Figure 8
Schematic diagram of a load displacement curve during nanoindentation[27].

The nanoindenter generates a load displacement curve like the one shown in Figure 8. The loading part of the curve is assumed to contain both plastic and elastic deformation, while the unloading portion of the curve is assumed to be purely elastic. In addition to this curve, the indenter tip used is carefully characterized by generating an area function, which is just the cross sectional area of the tip in contact with a sample at a given depth. The contact area of the indentation is then simply the value of the area function at the contact depth. The hardness is given by maximum load divided by the contact area[27]. Hardness testing was done with a Berkovitch tip. Each indent was performed with a 2 second approach and a 2 second retreat with a 2000 μN load.

2.4 Chemical Analysis

Samples 1350, 1500, 1800 were sent for wet chemical analysis to Dirats Laboratories. Weight percent values were obtained for Cu, Zr, O, N, and Fe.

3. Results and Discussion

3.1 Microstructural Evolution

Cursory examination of the x-ray patterns obtained from different sample times demonstrated qualitatively the cyclic behavior observed by El-Eskandarany in $Cu_{33}Zr_{67}$[6]. These results are shown in Figure 9 through Figure 11. As can be seen in Figure 9 at 300 minutes mixing was not yet completed, as the peaks from the elemental phases are still present. By 600 minutes a nearly amorphous phase has been produced. Samples taken at 825, 1125, 1350, and 1800 are mostly crystalline. The x-ray scans exhibit peaks from a single FCC phase, with a lattice parameter of 4.56 Å. This compares well to the lattice parameter obtained by El-

Eskandarany of 4.55 Å. Scans at 600, 900, and 1500 minutes appear to be predominately amorphous. Qualitatively the sample seems to be cycling between the FCC phase and an amorphous phase with a period of roughly 300 minutes. This is much faster than the 3000 minute period observed by El-Eskandarany, indicating that the process may have been of much higher intensity; however, the cyclic transformations were observed so the intensity estimation was close enough. On the 1125 and 1350 scans a small peak is resolved between 42 and 44 degrees. The identity of this peak was never verified. It does not correspond to any equilibrium oxide or nitride phases of Cu, Zr, or Fe, nor any intermetallics of these phases.

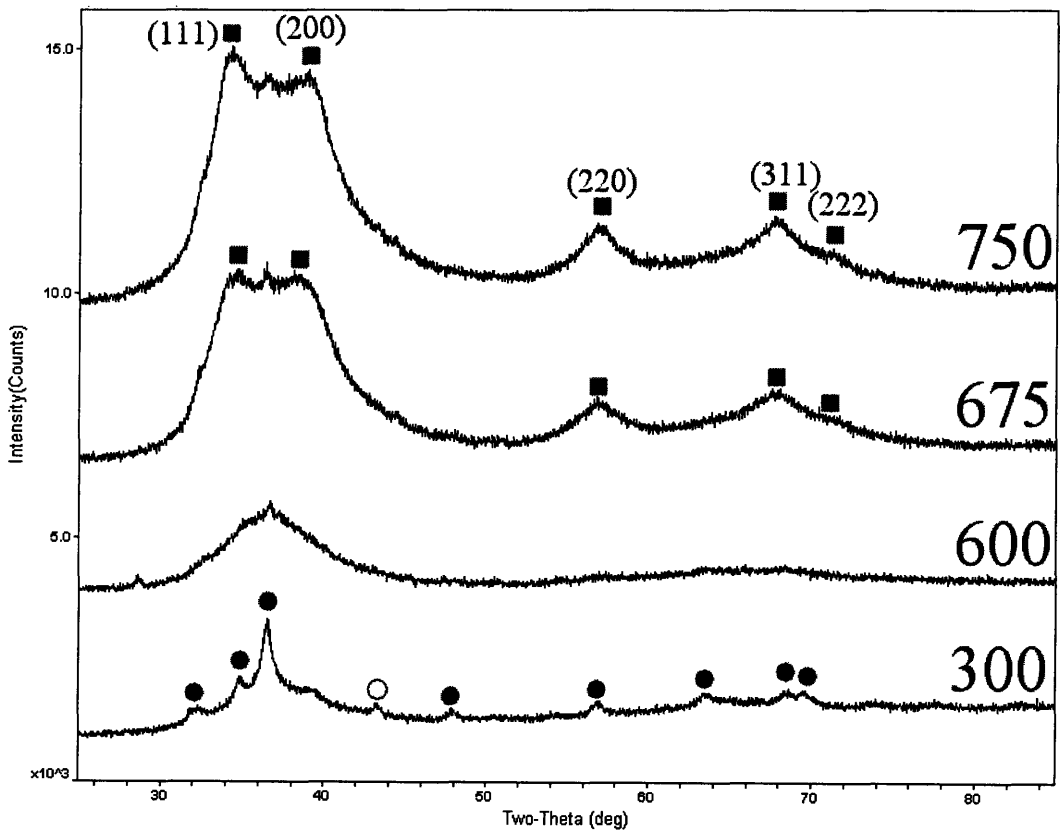

Figure 9
X-ray scans obtained for samples run at 300, 600, 675 and 750 minutes. Dark squares label the peaks of the FCC Cu-Zr phase. On the scan from 300 minutes dark circles label the crystal peaks from elemental HCP Zr, while the light circle labels the (111) peak from FCC Cu.

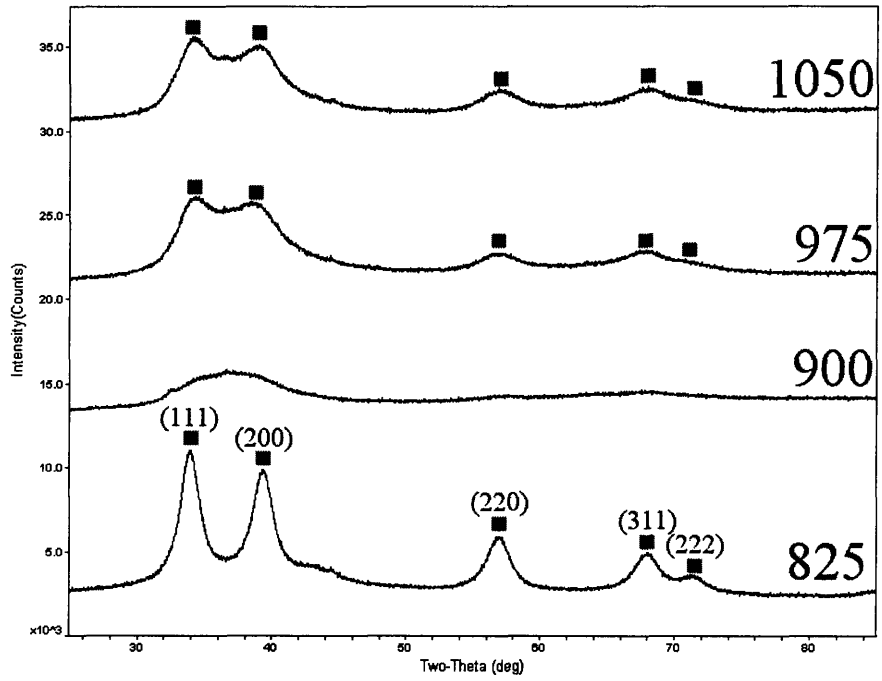

Figure 10
X-ray scans obtained for samples run at 825, 900, 975 and 1050 minutes. Dark squares label the peaks of the FCC Cu-Zr phase.

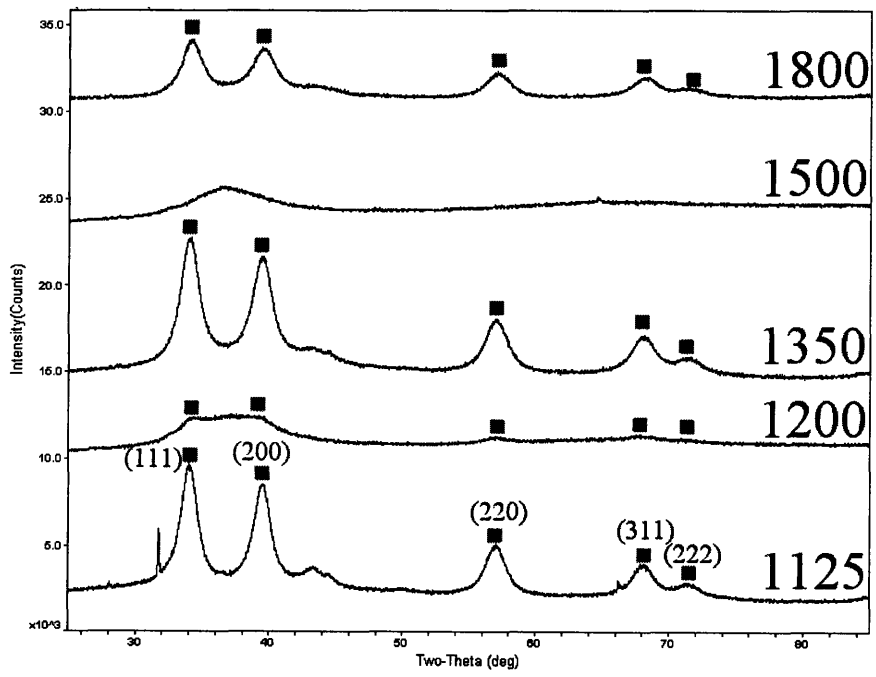

Figure 11
X-ray scans obtained for samples run at 1125, 1200, 1350, 1500, and 1800 minutes. Dark squares label the peaks of the FCC Cu-Zr phase.

More sophisticated x-ray analysis confirms this qualitative examination. On the mostly crystalline samples, 825, 1125, 1350, and 1800, simple peak decomposition was performed using Psuedo-Voight peak shapes for each of the FCC peaks and the two broad amorphous peaks. For the samples with more significant amorphous fractions Reitveld analysis was necessary in order to decompose the highly overlapped peaks. An FCC Zr phase with a modified lattice parameter of 4.57 used for the initial peak positions, and the background was estimated by hand. Subsequent refinement steps involved adding an amorphous peak at 35 degrees, then a second at 64, and finally allowing the background to be refined. Reitveld analysis would also have been used for the crystalline scans, but it requires detailed structural information unavailable for the metastable FCC Cu_xZr_y observed. While the data used for the FCC Zr phase was a close match, the method was unable to obtain very good fits for the very crystalline scans. The analysis was also unnecessary for these scans since the peaks were not badly overlapped. The subsequent Cocco and Schifinni analysis was performed and the values obtained for the amorphous fraction are tabulated in Table 1.

Time (min)	% Crystallinity
600	12.85
675	67.81
750	66.40
825	83.33
900	32.29
975	69.50
1050	70.06
1125	100.00
1200	52.55
1350	85.47
1500	0.00
1800	81.30

Table 1
The percent crystallinity of samples processed for different times.

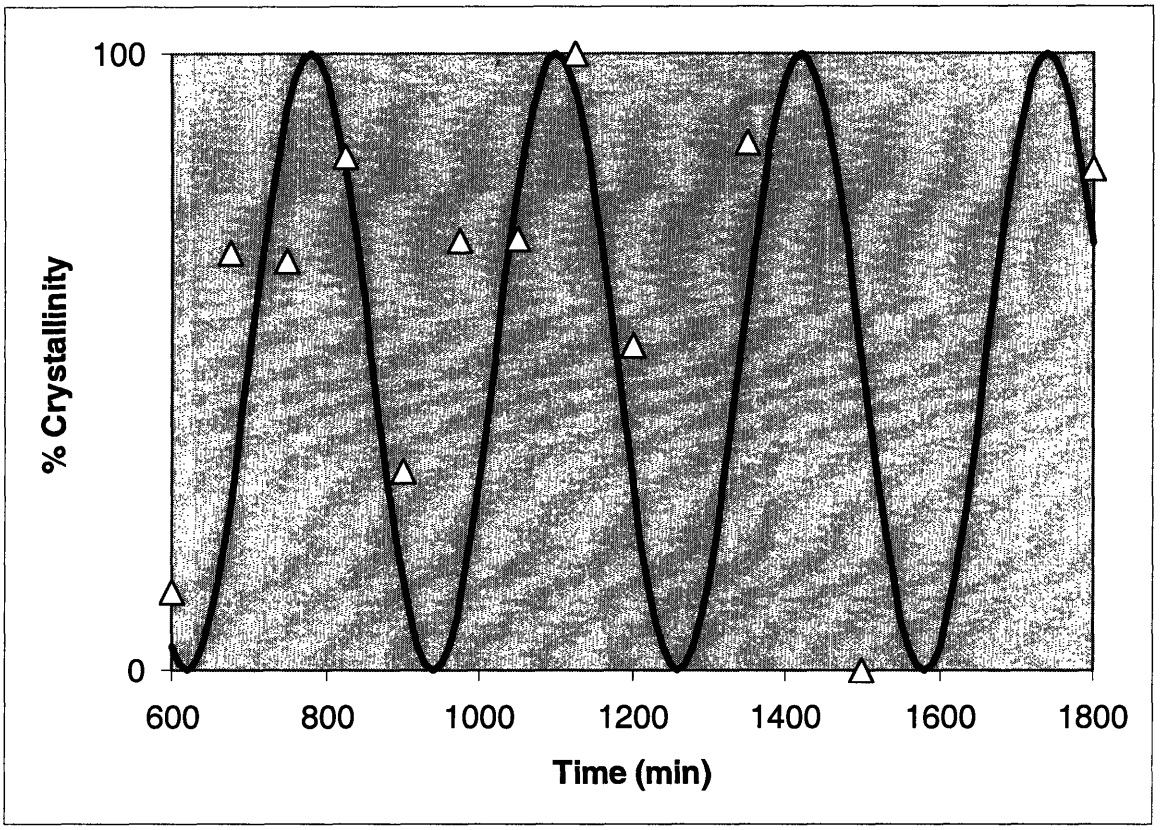

Figure 12
The triangles are the % crystallinity for the given processing times. The solid line is a sin wave with a period of 320 minutes and is included for visual reference.

Figure 12 shows the values plotted against a sine wave with a period of 320 minutes. It can be seen that the cycle qualitatively observed from the x-ray scans is confirmed by more sophisticated analysis. The exact pattern of the oscillation is still fairly obscure, more data points would be very helpful.

3.2 Hardness Evolution

Figure 13 illustrates the results obtained from the hardness testing. The average values of the all the hardness measurements for each time are represented by the dots, they range from 6.41 GPa to 10.47 GPa. The solid line is simply a sine wave with a period of 320 minutes;

however, when the data is compared to it can be seen that the hardness cycles between these two extreme values with a period similar to that of the sine wave.

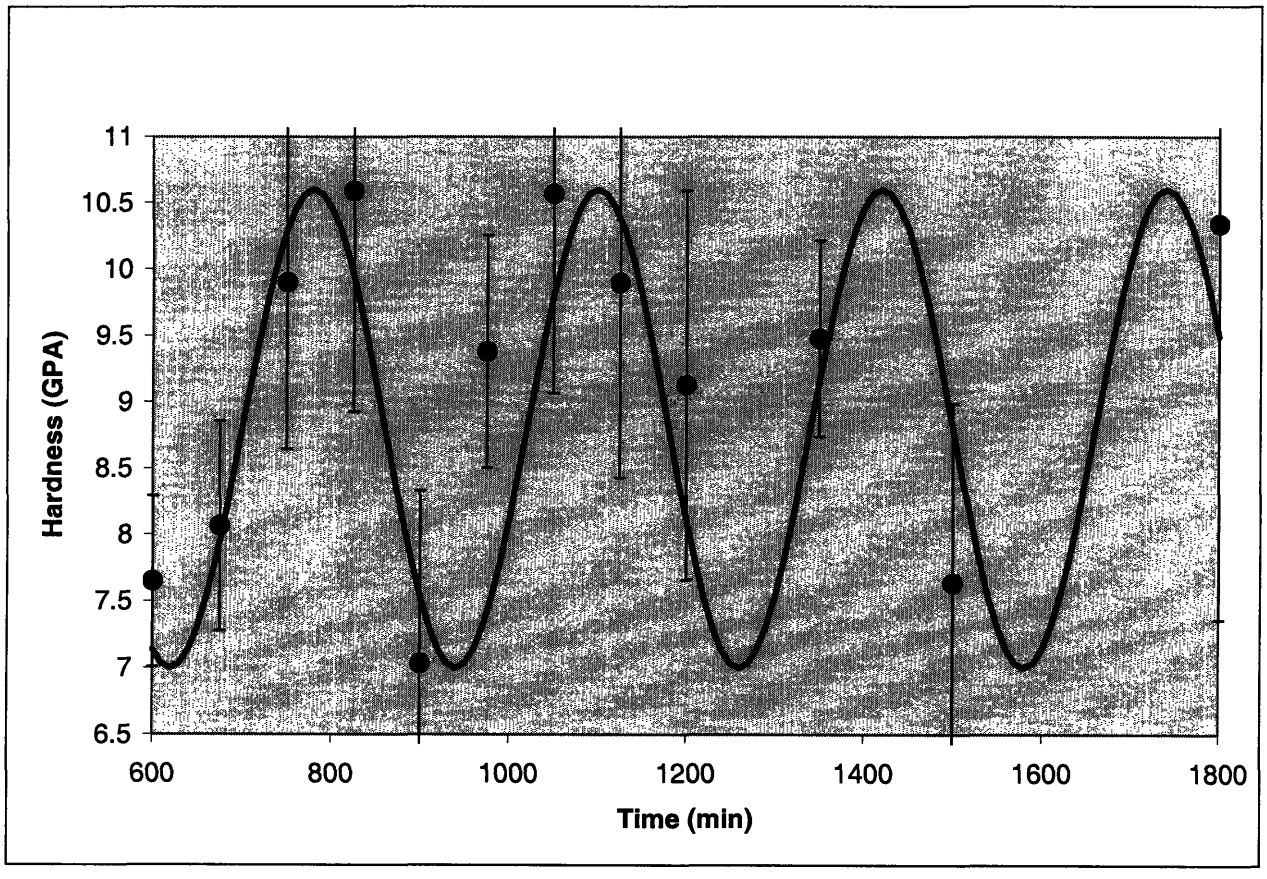

Figure 13
The dots are the obtained hardness values for the given processing times. The solid line is a sin wave with a period of 320 minutes and is included for visual reference.

The standard deviation of the measured hardness values is shown by the error bars on Figure 13. It is comparable to the magnitude of the variation in the hardness from time to time. Closer analysis of the hardness data reveals a possible explanation for this large deviation. The samples were mounted in an epoxy resin, with a modulus much lower than that of the powders. The powders ranged in diameter from between 10 microns to more than 50. Each indent was performed using 2000 μN force. Assuming that the contact area of the powders with the epoxy was roughly circular, the epoxy would have felt a pressure of 6 MPa for the smallest particles,

and 250 KPa for the larger ones. A pressure of 6MPa could be enough to deform the epoxy resin enough to interfere with the hardness test. In order to account for this problem, tests taken on the smaller powder particles can be removed from the data set.

Time(min)	Average Hardness(GPa)	Standard Deviation (GPa)
600	7.53	0.64
675	8.07	0.79
750	9.48	1.26
825	10.54	1.66
900	6.42	1.30
975	9.06	0.88
1050	10.24	1.50
1125	9.23	1.47
1200	8.51	1.47
1350	9.26	0.74
1500	7.06	1.35
1800	10.76	2.98

Table 2
The average values of the measured hardness at each time and the standard deviations of the measurements.

As can be seen from Figure 14, after this suspect data has been removed the standard deviation of the new set of measurements is much smaller than before, but the same cyclic hardness behavior is observed. It must be kept in mind that in biasing the data set towards larger particles, real variation in the hardness might be overlooked. Smaller particles could possibly have a different hardness than the larger ones; however the sample preparation would have to be performed differently in order to obtain values for their hardness.

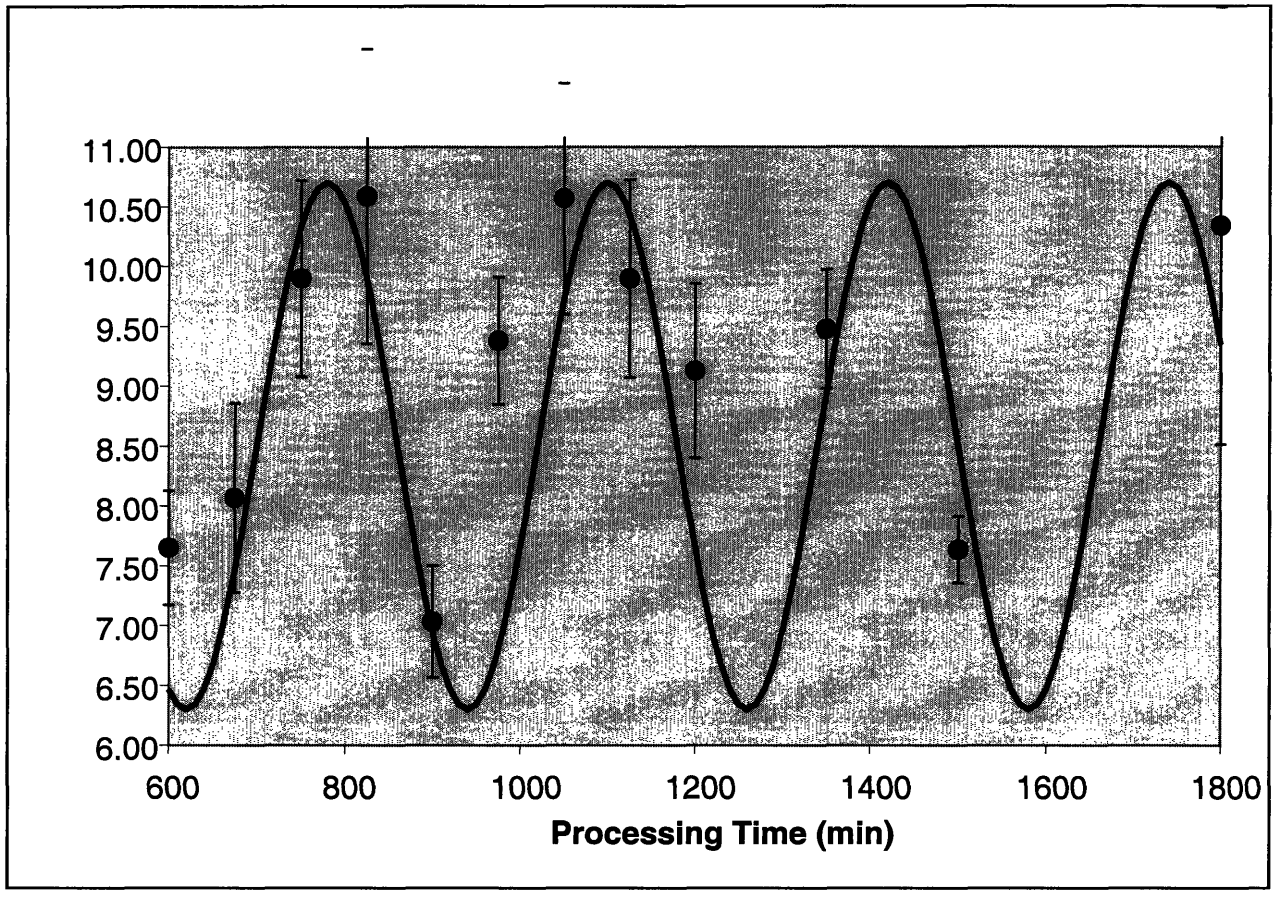

Figure 14
Hardness data with the data obtained from tests on smaller particles removed. The standard deviations of the data for each data point are shown as error bars.

3.3 Micostructure and Hardness Correlation

The percent crystallinity and the hardness were both observed to cycle each with a period of approximately 320 minutes. Figure 15 is a plot of percent crystallinity versus hardness. As expected there is a correlation between hardness and percent crystallinity. More amorphous samples are in general softer than the nanocrystalline FCC material.

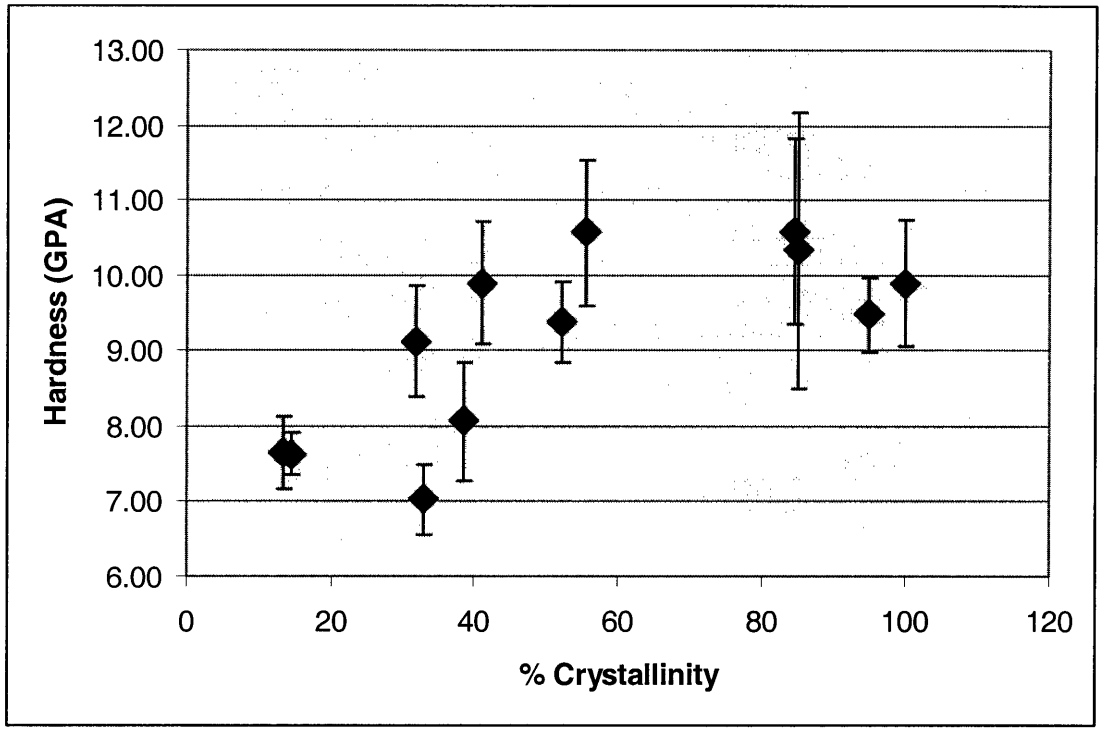

Figure 15
The hardness values for each sample are plotted against their percent crystallinity as obtained from x-ray diffraction analysis. The error bars are the standard deviations of the hardness measurements for each point.

3.4 Chemical Analysis

The wet chemical analysis found a large amount of chemical contamination in the samples. The combined samples taken at 1800 and 1500 minutes which were packed in high purity argon then milled in a sealed vial were reported to be 5.6 atomic percent oxygen, 10.2 atomic percent nitrogen, and 0.96 atomic percent iron. For the sample taken at 1350 minutes which was packed in high purity nitrogen there was reported to be 10.8 atomic percent oxygen, 27.7 atomic percent nitrogen, and 2.3 atomic percent iron.

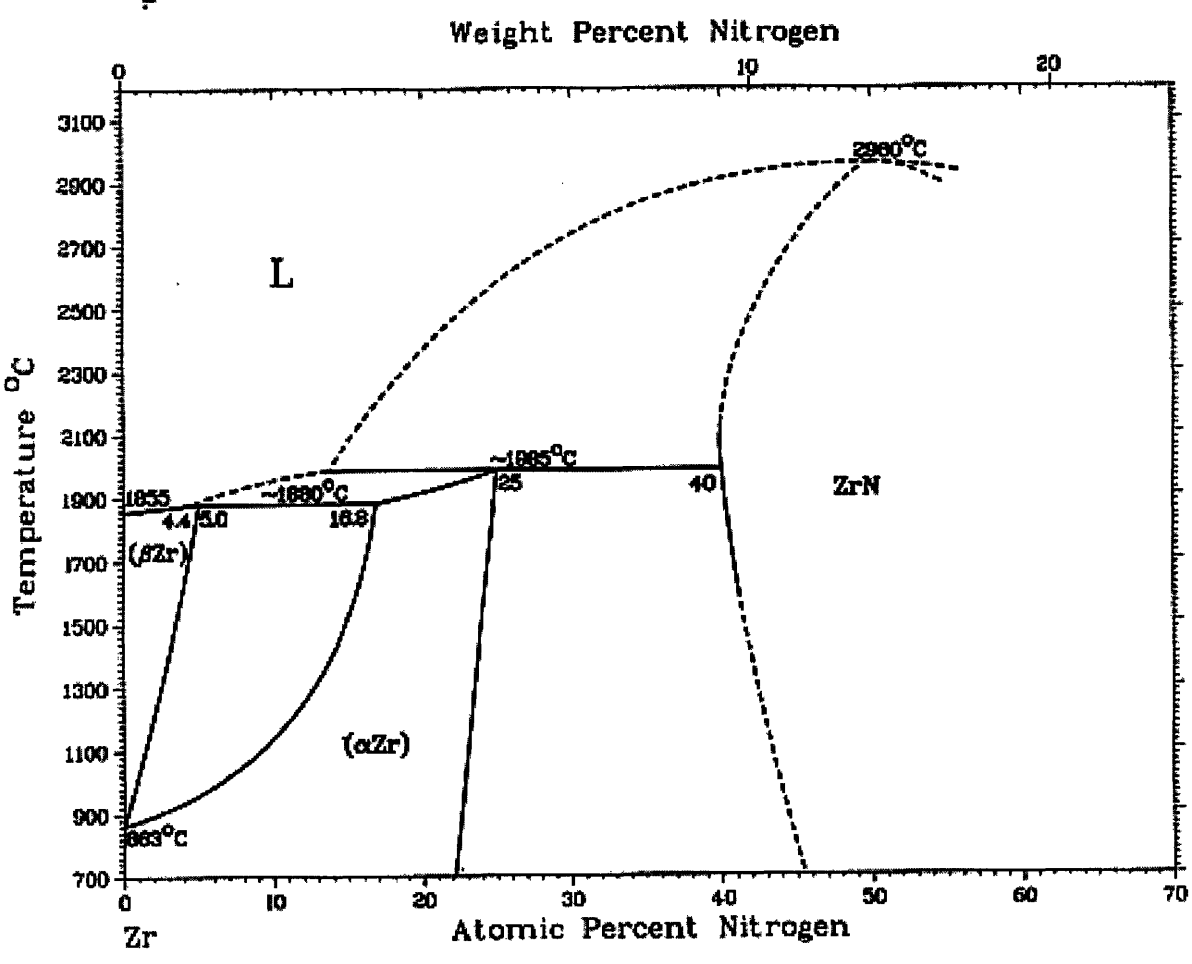

Figure 16
Binary phase diagram of zirconium and nitrogen[28].

These contamination values are very high. They would have been surprisingly high had the samples been milled in air. The amount of nitrogen present in the sample is well above nitrogen's solubility limit in zirconium at 700 °C, as can be seen from Figure 16, the zirconium nitrogen phase diagram. The solubility of oxygen and nitrogen in copper is negligible at room temperature.

These contamination values would be appropriate were there large fractions of oxide and nitride phases present; however, no such phases were observed in the x-ray diffraction patterns. The only phases observed are the amorphous fraction, and the FCC Cu-Zr solid solution. These

results are at least physically plausible, since extended solid solubility has been reported in several systems during mechanical alloying[29]; however, they indicate that the precautions taken to limit chemical contamination were entirely ineffective.

There are at least two possible sources for this extreme level of contamination. First, the seals on the vials may have been entirely compromised, so the experiment was essentially carried out in air. This, in point of fact, must have been the case if these values are true. The samples submitted for chemical analysis were approximately 1.5 g. They were reported to be 7.03 percent nitrogen, by weight. This would be equivalent to 169 mL of gaseous nitrogen, which is several times the volume of the vial used.

The high levels of iron contamination might be explained by oxidation on the inside surface of the vial. In between each test vials were cleaned in soapy water in an ultrasonic cleanser. There could have been some oxidation of the iron surface on the inside of the vials during this process, and this iron oxide would most likely have flaked into the sample during subsequent ball milling.

It is also possible that the results obtained were incorrect. In any case, the chemical composition of the processed samples is suspect given this disappointing chemical analysis. Such high levels of chemical contamination could have affected the test in a number of ways. The kinetics of phase transformation could have been significantly affected: this might explain why the period of the cyclic change observed was so much faster than that observed in the literature. It may also have had an effect on the hardness results. The cyclic transformation has been observed without this level of contamination though, and since the phases observed in this study match the phases observed in the literature it is reasonable to suppose that this is the same sort of cyclic transformation. Even though the contamination may have changed the hardness

values from what they would have been without it, there is no reason to suppose that this contamination would have affected the hardness in a cyclic manner.

3.5 Discussion of Importance for Mechanical Alloying Theory

The samples were found to be heavily contaminated with both oxygen and nitrogen. This discovery renders the results obtained somewhat ambiguous. The contamination may have significantly affected the phase transformations observed as well as the hardness values obtained; however, the phases observed were the same as those observed in previous studies of mechanical alloying in this system. The cyclic transformations have been observed by other authors' without contamination and there is no reason to believe the hardness variation would not also be observed.

The observation of a hardness cycle along with the percent crystallinity cycle has implications for an explanation of the cyclic phase transformations, although it is by no means definitive. The model offered in 1998 by Sluiter and Kawazoe[22] which suggested the build up of defects which catalyzed the phase transformation is certainly not inconsistent with a cycle in the hardness. It is not clear that this model would necessarily suggest a cycle like the one observed. These observations do little to support or undermine that model; however, at the authors' own admission the model faces problems for other reasons.

These observations do help to lend support to an explanation of the cyclic transformation in terms of a concomitant cycle in processing intensity. As stated in the review, it has been widely observed that phases obtained during mechanical alloying processes depend strongly on the relevant processing intensity. There is also a good deal of evidence that the relevant intensity is proportional to the power of the process[7]. In the model used for setting the intensity of the

process in a SPEX mill, the parameters involved the ball size, the ball to powder weight ratio, and the filling fraction of the vial. This model assumes the power is equal to the energy of each collision divided by the frequency of collisions. A key assumption of the model is that the collisions are perfectly inelastic so that all the incident kinetic energy of the ball goes into the collision.

The model does not take into account the mechanical properties of the powders being processed. This consideration is not important when the powder's properties do not vary; however, in at least this case one relevant property, the hardness, is varying. It seems much more reasonable that the relevant intensity would depend not just on the power going into the collisions, but rather how much power is actually being absorbed by the powder. Harder powders should absorb less energy for each impact, and hence feel a lower intensity than softer powders, holding all other processing parameters constant. Using the language of driven alloy theory, for the same process, harder powders will feel a lower effective temperature.

Without a phase map across effective temperatures this line of reasoning alone is really insufficient to explain the cyclic transformation from the cyclic hardness and processing intensity. In order for driven alloy theory to offer an explanation, the crystalline phase would need to be stable at higher effective temperatures and the amorphous phase at lower effective temperatures. At first glance this seems reversed from what might be expected. There is some reason to believe that this is in point of fact the case.

The crystalline phase obtained is metastable and highly nonequilibrium, so it is not absurd to imagine it is a less stable phase than the amorphous one. It has been observed that at lower processing intensities the cyclic phenomena does not occur. Instead, an amorphous phase is formed with no subsequent transformations[6]. This is consistent with what would be expected

were the cycles due to a change in effective temperature. One would also expect to observe that at higher processing intensities a crystalline phase which does not cycle would be observed. This has not been experimentally verified, to this author's knowledge.

A simple appeal to effective temperature is also insufficient to explain the cycling because for a given process, there should be some pair of effective temperature and powder hardness in which the system is in dynamic equilibrium. When the powder is fully amorphous, the effective temperature will be high, promoting the creation of the crystalline phase. As the percent crystallinity increases, the effective temperature lowers. The phase composition seems to change continuously, so the powder should move through the dynamic equilibrium point. There must be some reason the phase composition continues to shift beyond this dynamic equilibrium point.

At least one possible explanation is that the hardness does not fully correlate with the percent crystallinity. Some other change in the microstructure independent of the phase transformations, such as change in the grain size of the crystalline phase, could influence the hardness as well. This might provide a driving force to change the hardness and therefore effective temperature in a powder which is in dynamic phase equilibrium at the current effective temperature of the vial.

This prediction is consistent with the observed behavior of the hardness with varying amorphous fraction. Although the data is not complete enough to clearly show any particular variation of the hardness with amorphous fraction other than a vaguely linear one, the sample taken at 900 minutes which is 32% crystalline is softer than the sample taken at 1500 minutes which is fully amorphous. The fully crystalline taken at 1125 minutes is softer than the only party crystalline samples taken at 1050 and 825 minutes.

These comments are conjectural and do not constitute an alternative model to the defect accumulation model considered; however, it does seem quite plausible from the data obtained that hardness variations may have an important role to play in the cyclic transformation, and an appeal to ball milling as a driven alloy process may very well explain how.

4. Conclusions

This study was undertaken to investigate the cyclic transformations that have been observed in ball milling experiments in some two component systems. The system chosen for study was $Cu_{33}Zr_{66}$. Cyclic transformations have been observed in this system in another study, and the experiment was designed to duplicate as nearly as possible the conditions of that study. Values for the percent crystallinity and hardness were obtained as a function of processing time.

In a SPEX 8000M shaker mill, using 4.76 mm diameter hardened tool steel balls in a hardened tool steel vial, with less than a 1:10 filling fraction, $Cu_{33}Zr_{66}$ powders were observed to cycle between an amorphous phase and an FCC Cu-Zr phase with a lattice parameter of 4.56 Å. These cycles occurred with a period of approximately 320 minutes. The hardness of the powders cycled between approximately 6.5 GPa and 10.5 GPa with a similar period. A rough correlation between percent cyrstallinity and hardness was also observed.

The observed cycling of the hardness values with the percent crystallinity values help to support an explanation of the cyclic transformations in terms of changing process intensity. In the language of driven alloy theory, the hardness of the powders may change the effective temperature of the process for the same set of other processing variables. This changing effective temperature may promote the formation of one phase rather than another, but this newly formed phase will have a different hardness and therefore experience a different effective

temperature, which could then promote the formation of the first phase. A large amount of elaboration will be required to form this idea into a model, and several problems need to be addressed.

This study also suggests more experimental work which could be done. The most pressing work simply involves improving the data collected in the current investigation. The data set would be far more convincing if the chemical contamination problems were addressed. The best way to accomplish this would be to run the milling experiments entirely in a controlled atmosphere, rather than simply packing and sealing the vials in a controlled atmosphere. This would prevent any contamination due to a poor seal on the vial. The data set would also be helped substantially by significantly more data points. The quality of the hardness measurements would be increased by many more data points, and the x-ray analysis can be improved by longer slower scans.

Investigating the cyclic transformations at different intensities and longer times would also reveal useful information. Running the process at much higher intensities, by using larger milling balls, would also be very interesting if there were a critical processing intensity above which the cycling process no longer occurred. This would lend more plausibility to the explanation for the cyclic transformation offered; as it would provide evidence that the FCC phase was indeed stable at higher effective temperatures than the amorphous one. There is also a very important question to address as to whether the cycles will continue indefinitely, or whether they will dampen to a steady state. This will have very important implications for any model offered to explain the phenomenon. This question can really only be answered by running the process for much longer times, and observing very carefully the variation in percent crystallinity over time.

Ball milling is not the only mechanical alloying process; however, cyclic phase transformations have not been observed in other processes. It would be interesting to know whether the cyclic transformations are simply a feature intrinsic to phase changes during any mechanical alloying process, or whether they are a phenomenon which only occurs during ball milling. In addition to helping to reveal the importance of the cyclic transformations, this knowledge would also help guide the formation of models.

Although the study was not definitive and the results are given with some reservation, the cyclic phase transformations were observed in addition to a cycle in the hardness of the milled powders. A great deal of experimental and theoretical work needs to be done before the phenomenon can be completely explained, but this study helps to point the direction towards that work.

References

[1] Suryanarayana, C. *Progress in Materials Science*. 46, 1-184. 2001.
[2] Li, F; Ishihara, KN; Shingu, PH; *Metallurgical Transactions*. 36, 123-8. 1998.
[3] Lund, A; Schuh, C; *Journal of Applied Physics*. 95(9), 4185-4822. May 2004.
[4] Eckert, J; Holzer, JC; Krill III, CE; Johnson, WL. *Materials Science Forum*. v88-90, p505-12. 1992.
[5] Martin, G; Bellon, P. *Solid State Physics*. 50, p189. 1997.
[6] El-Eskandarany, M; Inoue, A. Metallurgical and Materials Transactions A – Physical Metallurgy and Materials Science. 33(7), 2145-2153. July 2002.
[7] Gaffet, E. *Materials Science and Engineering Part A*. 132, p181-193. 1991.
[8] Watanabe, R; Hashimoto, H; Lee GG. *Materials Transactions JIM*. 36, p161-169. 1995.
[9] Koch, CC; Davis, RM. *Scripta Metallurgica*. 21, p305-310. 1987.
[10] Kock, CC. *International Journal of Mechanochemical and Mechanical Alloying*. 1, p 56-67. 1994.
[11] Magini, M; Burgio, N; Iasonna, A; Martelli, S; Padella, F; Paradiso, E. *Journal of Materials Synthesis and Processing*. 1, p135-144. 1993.
[12] Abdellaoui, M; Gaffet, E. *Acta Metallurigca Materialia*. 43, p1087-1098. 1995.
[13] Murty BS; Ranganathan, S. *International Materials Reviews*. 43(3) p101-141. 1998.
[14] El-Eskandarany, M; Aoki, M, Sumiyma, K; Suzuki, K. *Applied Physics Letters*. 70, p1679. 1997.
[15] El-Eskandarany, M; Aoki, K; Sumiyma, K; Suzuki, K. *Acta Materialia*. 50, p1113-1123. 2002.
[16] El-Eskandarany, M; Aoki, K; Sumiyama, K; Suzuki, K. *Scripta Materialia*. 36, p1001. 1997.
[17] El-Eskandarany, M; Inoue, A. *Metallurical and Materials Transactions A*. 33(1), p135-143. 2002.
[18] Huang, JY; Wu, YK; Ye, HQ. *Acta Metallurica*. 44, p1201. 1996.
[19] El-Eskandarany, M; Saida, J; Inoue, A. *Acta Materialia*. 51(15), p4519-4532. 2003.
[20] Morris, MA; Morris, DG. *Materials Science Forum*. 88-90, p529. 1992.
[21] Cocco, G; Soletta, I; Battezzati, L; Baricco, M; Enzo, S. *Philosophical Magazine B*. 61, p473-479. 1990.
[22] Sluiter, M; Kawazoe, Y. *Acta Materialia*. 47(2), p475-480.
[23] Atzmon, M; Xu, J; Tian, HH. *Materials Science Forum*. v360-362, p311-316. 2001.
[24] Magini, M; Iasonna A. *Materials Transactions JIM*. 36(2), 123-133. February, 1995.
[25] Lutterorotti, L; Ceccato, R; Dal Maschio, R; Pagini, E. *Materials Science Forum*. 278-281, p87. 1998.
[26] Delogu, F; Schiffini, L; Cocco, G. *Philosophical Magazine A*. 81(8), 1917-1937. August, 2001.
[27] Oliver, WC; Pharr, GM. *Journal of Materials Research*. 19(1), 3-20. 2004.
[28] ASM International. *Binary Alloy Phase Diagrams*. Vol 3. 1990.
[29] Huang, BL; Perez, RJ; Lavernia, EJ; Luton, MJ. *Nanostructured Materials*. 7, p67-79. 1996.